A Nickel Tripeptide as a Metallodithiolate Ligand Anchor for Resin-Bound Organometallics

Kayla N. Green, Stephen P. Jeffery, Joseph H. Reibenspies, and
Marcetta Y. Darensbourg*

*Contribution from the Department of Chemistry, Texas A&M University,
College Station, Texas 77843-3255*

Received February 13, 2006; E-mail: marcetta@mail.chem.tamu.edu

Abstract: The molecular structure of the acetyl CoA synthase enzyme has clarified the role of individual nickel atoms in the dinickel active site which mediates C−C and C−S coupling reactions. The NiN_2S_2 portion of the biocatalyst (N_2S_2 = a cysteine-glycine-cysteine or CGC^{4-} tripeptide ligand) serves as an S-donor ligand comparable to classical bidentate ligands operative in organometallic chemistry, ligating the second nickel which is redox and catalytically active. Inspired by this biological catalyst, the synthesis of NiN_2S_2 metalloligands, including the solid-phase synthesis of resin-bound $Ni(CGC)^{2-}$, and sulfur-based derivatization with $W(CO)_5$ and $Rh(CO)_2^+$ have been carried out. Through comparison to analogous well-characterized, solution-phase complexes, Attenuated Total Reflectance FTIR spectroscopy establishes the presence of unique heterobimetallic complexes, of the form $[Ni(CGC)]M(CO)_x$, both in solution and immobilized on resin beads. This work provides the initial step toward exploitation of such an evolutionarily optimized nickel peptide as a solid support anchor for hybrid bioinorganic−organometallic catalysts.

Introduction

With the discovery of the dinickel site in the acetyl CoA synthase (ACS) metalloenzyme (Figure 1), a new paradigm for di- and polymetallic enzyme active site construction has been recognized. In this case, one nickel is incorporated into a Cys-Gly-Cys tripeptide motif, bound by two carboxyamido nitrogens of a cysteine and the glycine, along with the sulfurs of both cysteines, in a secure, square-planar N_2S_2 coordination site.[1−3] The cysteinyl sulfur atoms in turn capture a second nickel ion whose coordination environment is well-suited for the organometallic reactions required of the ACS enzymatic cycle which include oxidative addition of CH_3^+, methyl-CO migratory insertion, and reductive elimination of $RSC(=O)R'$.[4] It has been suggested, and corroborated by computational chemistry, that the NiN_2S_2 portion of the active site may be considered as a supporting ligand, capable of stabilizing the second nickel in a low-valent redox level required for the oxidative addition of Me^+.[4] Another possible advantage of the NiN_2S_2 metalloligand in the ACS active site is its hemilabile, ring-opening property which generates an open site on the catalytic metal.[5]

Interestingly there is a passage between ACS and its partner, carbon monoxide dehydrogenase (CODH), in the form of a hydrophobic channel through which CO is directed from its site
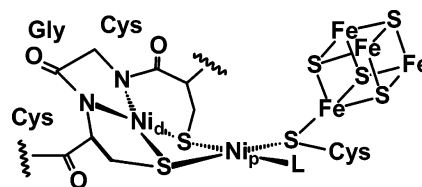

Figure 1. Representation of the A-cluster active site of acetyl CoA synthase.[2]

of production in CODH to its site of utilization in ACS.[2] While the evolutionary design in proteins produces channels through protein folding, synthetic chemists may crudely mimic such isolated catalyst sites by embedding active site mimics in solid supports.[6] Semiporous resin beads with solvent channels or microdomains formed by lengthy poly(ethylene glycol) chains permit attached catalyst site isolation with possibilities for substrate size recognition.[6−11] The goal of the work described below is to lay the foundation for the use of natural metallopeptides as resin-bound ligands for potentially catalytically active metals.

The structures of numerous inorganic polymetallic compounds confirm the notion that NiN_2S_2 complexes may be considered as molecular construction units whose S-based aggregation

(1) Doukov, T. I.; Iverson, T. M.; Seravalli, J.; Ragsdale, S. W.; Drennan, C. L. *Science* **2002**, *298*, 567−572.
(2) Darnault, C.; Volbeda, A.; Kim, E. J.; Legrand, P.; Vernède, X.; Lindahl, P. A.; Fontecilla-Camps, J. C. *Nat. Struct. Biol.* **2003**, *10*, 271−279.
(3) Amara, P.; Volbeda, A.; Fontecilla-Camps, J. C.; Field, M. *J. Am. Chem. Soc.* **2005**, *127*, 2776−2784.
(4) Webster, C. E.; Darensbourg, M. Y.; Lindahl, P. A.; Hall, M. B. *J. Am. Chem. Soc.* **2004**, *126*, 3410−3411.
(5) Phelps, A. L.; Rampersad, M. V.; Fitch, S. B.; Darensbourg, M. Y.; Darensbourg, D. J. *Inorg. Chem.* **2006**, *45*, 119−126.

(6) Grubbs, R. H.; Kroll, L. C. *J. Am. Chem. Soc.* **1971**, *93*, 3062−3063.
(7) Sherrington, D. C. *Chem. Commun.* **1998**, 275−2286.
(8) Ford, W. T.; Bergbreiter, D. E.; Waller, F. J.; Ekerdt, J. G.; Garrou, P. E.; Neckers, D. C.; Taylor, R. T.; Wulff, G.; Patchornick, A.; Nov, E.; Jacobson, K. A.; Shai, Y. *Polymer Reagents and Catalysts*; ACS Symposium Series 308; American Chemical Society: Washington, DC, 1986; pp 1−17, 84−106, 247−285.
(9) Kunquan, Y.; McKittrick, M. W.; Jones, C. W. *Organometallics* **23**, 4089−4096.
(10) Annis, D. A.; Jacobsen, E. N. *J. Am. Chem. Soc.* **1999**, *121*, 4147−4154.
(11) Leadbeater, N. *J. Org. Chem.* **2001**, *66*, 2168−2170.

properties can lead to unique, albeit largely unreactive, clusters.[12−14] This aggregative tendency can be controlled by use of interacting electrophiles with low affinity for sulfur or by steric blocks. The latter reaches a pinnacle in catalyst site isolation found in proteins, as demonstrated by the ACS active site.
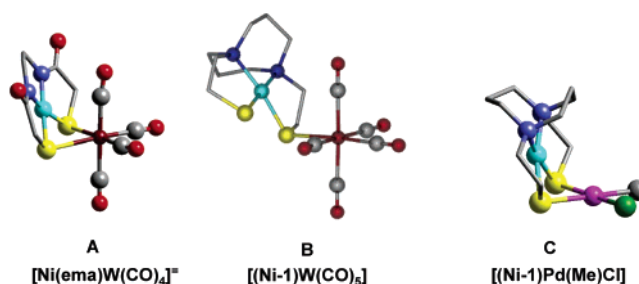
Small molecule models of metalloenzyme active sites are valuable as synthetic analogues of inorganic or organometallic natural products with the potential for catalytic activity.[15] From an array of di- and tetraanionic tetradentate N_2S_2 ligands bound to nickel(II) we have established the following fundamental properties of NiN_2S_2 complexes as metalloligands: (1) They are good electron donors as established by the ν(CO) spectroscopy of W(CO)$_4$ derivatives;[15] (2) NiN_2S_2 complexes can bind as mono- or bidentate ligands, a property fundamental to hemilability;[5,15] (3) the additional lone pair on each sulfur donor site imposes an asymmetrical feature to this ligand quite unlike other planar ligands. This steric feature is expressed in terms of a hinge angle defined by the NiN_2S_2 plane with respect to the binding site of the exogenous metal. Most important to our studies is the ν(CO) spectroscopy of tungsten carbonyl derivatives which can be used to identify NiN_2S_2 ligands. With this database, we can demonstrate that the naturally optimized Ni(CGC)$^{2-}$ ligand of acetyl CoA synthase behaves as a typical NiN_2S_2 ligand to W(CO)$_x$ moieties ($x = 4, 5$) and it can also serve as an anchor for organometallics to polystyrene resin beads. Through Attenuated Total Reflection Fourier Transform Infrared Spectroscopy, ATR-FTIR, the solid-supported Ni(CGC)$^{2-}$ is readily detectable as metal-carbonyl derivatives matching assignments of ν(CO) vibrational spectra to solution phase analogues. Such an Aufbau of characterization permits extensions to other resin-bound hybrid biological/organometallic moieties with the potential as isolated single site catalysts, e.g., {Ni(CGC)Rh(CO)$_2$$^-$}.

Methods and Materials

General. (Abbreviations for ligands used are found in Chart 1.) Solvents were reagent grade and were purified according to standard procedures.[16] The **Ni-1** (see Chart 1), K$_2$[Ni(CGC)] and *cis*-(pip)$_2$W-(CO)$_4$ (pip = piperidine) complexes were prepared as described.[17−19] Other reagents were purchased from commercial sources and used as received unless noted. Syntheses of air-sensitive Ni(II) complexes were performed under anaerobic conditions using distilled/degassed solvents and standard Schlenk line techniques under an argon atmosphere. The preparation of K$_2$[Ni(CGC)W(CO)$_4$] and K$_2$[Ni(CGC)W(CO)$_5$] followed procedures developed for neutral NiN_2S_2 ligands.[5,15]

Standard Fmoc Merrifield techniques were employed for all peptide syntheses. The solid supports, TentaGel-S RAM Fmoc resin-beads (Advanced Chem Tech) averaging 90 μm in diameter, are composed of polystyrene with cross-linking via divinylbenzene and grafted with poly(ethylene glycol) bearing a Rink linker (trialkoxybenzhydrylamine)

(12) Golden, M. L.; Rampersad, M. V.; Reibenspies, J. H.; Darensbourg, M. Y. *Chem. Commun.* **2003**, 1824−1825.
(13) Jeffery, S. P.; Lee, J.; Darensbourg, M. Y. *Chem. Commun.* **2005**, 1122−1124.
(14) Rao, P. V.; Bhaduri, S.; Jiang, J.; Holm, R. H. *Inorg. Chem.* **2004**, *43*, 5833−5849.
(15) Rampersad, M. V.; Jeffery, S. P.; Golden, M. L.; Lee, J.; Reibenspies, J. H.; Darensbourg, D. J.; Darensbourg, M. Y. *J. Am. Chem. Soc.* **2005**, *127*, 17323−17334.
(16) Gordon, A. J.; Ford, R. A. *The Chemist's Companion*; Wiley and Sons: New York, 1972; pp 429−436.
(17) Mills, D.; Reibenspies, J. H.; Darensbourg, M. Y. *Inorg. Chem.* **1990**, *29*, 4366−4368.
(18) Krishnan, R.; Riordan, C. G. *J. Am. Chem. Soc.* **2004**, *126*, 4484−4485.
(19) Darensbourg, D. J.; Kump, R. L. *Inorg. Chem.* **1978**, *17*, 2680−2682.

Chart 1.[a]

A
[Ni(ema)W(CO)$_4$]$^-$

B
[(Ni-1)W(CO)$_5$]

C
[(Ni-1)Pd(Me)Cl]

[a] Abbreviations: Ni(ema)$^{2-}$ = nickel(II) (*N,N*′-ethylenebis-2-mercaptoacetamide); **Ni-1** = nickel(II) (*N,N*′-bis-2-mercaptoethyl-*N,N*′-diazocyclooctane).

as the free amine termini (0.4 mmol/g loading). Plastic-fritted syringes, 10 mL, were used as reaction vessels to facilitate the multiple additions and removal of reagents and wash solvents. Mixing of beads and reagents was accomplished by an automated shaker.

Solution infrared spectra were recorded on a Bruker Tensor 27 FTIR spectrometer using 0.1 mm NaCl sealed cells. The Pike MIRacle attachment from Pike Technologies was used for Attenuated Total Reflectance Infrared Spectra for solid-state samples. UV−vis spectra were recorded on a Hewlett-Packard HP8452A diode array spectrometer. Mass spectrometry (ESI-MS) was performed by the Laboratory for Biological Mass Spectrometry at Texas A&M University. Elemental analyses were performed by the Canadian Microanalytical Servies, Ltd., Delta, British Columbia, Canada.

Synthesis of Resin-Bound [Ni(CGC)]$^{2-}$. The N-acylated CysGly-Cys peptide was constructed on the TentaGel resin beads using standard Fmoc techniques. Deprotection of the Mmt (4-methoxytrityl) protected cysteine with minimal cleavage of the tripeptide from the resin was accomplished via a 1:94:5 mixture of trifluoroacetic acid/dichloromethane/triisopropylsilane. The solution was deployed in 5 mL aliquots at 5 min intervals until the deprotection mixture removed from the peptide-bound resins was no longer yellow, indicating removal of the cysteinyl Mmt thiol-protecting group. Following washes (3 × 5 mL each) with pure CH$_2$Cl$_2$ and MeOH solvents, a basic solution of green nickel acetylacetonate (25 mg, 0.1 mmol + 22 mg, 0.4 mmol KOH) in 5 mL of dichloromethane was introduced to the resin bed. The light-yellow color of the beads changed to a bright orange within 30 s. After 10 min, the solution containing the nickel source was removed, and the beads were again washed with CH$_2$Cl$_2$ solvent until the residual washes were completely colorless. The beads were dried in vacuo and stored in a vacuum desiccator. They were frequently handled in air with no apparent deleterious effects.

Synthesis of Resin-Bound Ni(CGC)M(CO)$_x$$^{n-}$, ○−Ni(CGC)W-(CO)$^{s2-}$, and ○−Ni(CGC)Rh(CO)$_2$$^{1-}$. A portion of ○−Ni(CGC)$^{2-}$, was placed in a syringe, and CH$_2$Cl$_2$ was used to swell the resin beads. A yellow solution of (pip)$_2$W(CO)$_4$ in CH$_2$Cl$_2$ was drawn up into the syringe, and the mixture was agitated for 10 min on an automated shaker. The color of the beads slowly changed from bright orange to burnt yellow. The beads were washed (6 × 10 mL CH$_2$Cl$_2$) and dried under a vacuum. ν(CO): 1967w, 1917s, 1850w cm^{-1}. An alternative route to the same product utilized (THF)W(CO)$_5$.

In the same way a red solution of (Rh(CO)$_2$Cl)$_2$ in MeOH/CH$_2$Cl$_2$ was exposed to the resin-bound nickel tripeptide. The resulting dark red beads after washing and drying had ν(CO) at 2067s and 1990s cm^{-1}.

Synthesis of [Et$_4$N]$_x$[Ni(ema)Rh(CO)$_2$]$_x$ ($x = 1,2$), Complex E. Under an Ar atmosphere, red solids (Rh(CO)$_2$Cl)$_2$, ν_{CO} (MeCN) 2097, 2026 cm^{-1}, (30 mg, 0.077 mmol) and (Et$_4$N)$_2$Ni(ema) (80 mg, 0.154 mmol) were dissolved in 25 mL of CH$_3$CN and stirred for 1 h and filtered through a Celite pad. A solid was obtained after precipitation with ether, and removal of supernatant fluid via cannula yielded a red/brown solid. Crude product yield was 0.0434 g (51%). Further

Table 1. CO Stretching Frequencies ($NiN_2S_2W(CO)_4$ in Dimethylformamide, DMF, and $NiN_2S_2W(CO)_5$ in Tetrahydrofuran, THF, Solvent) and Calculated Force Constants (FC) for the $W(CO)_x$ (x = 4, 5) Derivatives of the Tripeptide $Ni(CGC)^{2-}$ and the $Ni(ema)^{2-}$ Complex Ions[a]

$K_2[Ni(CGC)]$	1988w, 1863s, 1845sh, 1793ms cm^{-1}	2061w, 1974sh, 1917s, 1869m cm^{-1}
FC (mdyn/Å)	k_1 = 13.43, k_2 = 14.92, k_i = 0.45	k_1 = 15.55, k_2 = 14.28, k_i = 0.36
$[NEt_4]_2[Ni(ema)]$	1986w, 1867s, 1837sh, 1791m cm^{-1}	2060w, 1967sh, 1918s, 1868m cm^{-1}
FC (mdyn/Å)	k_1 = 13.41, k_2 = 14.77, k_i = 0.46	k_1 = 15.56, k_2 = 14.28, k_i = 0.35

[a] The vibrational mode assignments and the calculation of force constants are according to ref 20.
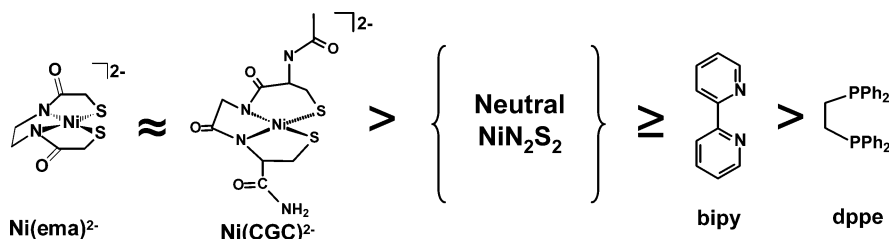
Figure 2. Rank of electron donor ability as evidenced by $(NiN_2S_2)W(CO)_4$ derivatives and their respective $\nu(CO)$ IR bands and force constants; see ref 16.

purification involved redissolving the solid in CH_3OH, precipitation with ether, and removal of the supernatant fluid followed by further washing with Et_2O. Due to air sensitivity, CO lability, and solvation proclivity, efforts to obtain analytically pure compound were not entirely successful. Crystals of crystallographic quality were obtained by layering the acetonitrile solution with ether. ESI-MS (MeCN): {[(Ni(ema)-Rh(CO)_2)]}$^-$ 420 (100%). $\nu(CO)$ (CH_3CN): 2061s, 1996s cm^{-1}. Anal. Calcd (found) for $[NEt_4]_2[Ni(ema)_2(Rh(CO)_2)_2]\cdot CH_3OH$ or $C_{33}H_{60}N_6$-$Ni_2O_9Rh_2S_4$: C, 34.88 (35.85); H, 5.32 (6.91); N, 7.40 (6.98).

Preparation of $[(Ni-1)Rh(CO)_2][PF_6]$, Complex D. Under Ar a sample of $[Rh(CO)_2Cl]_2$ (0.0281 g, 0.072 mmol) was dissolved in 5 mL of CH_3CN resulting in a pale yellow solution. In a separate flask, **Ni-1** (0.042 g, 0.144 mmol) and $TlPF_6$ (0.0503 g, 0.144 mmol) solids were mixed and dissolved in 10 mL of CH_3CN. Cannula transfer of the purple **Ni-1** solution to the Rh source resulted in immediate formation of an orange solution with a yellow precipitate of TlCl. Following 2 h of stirring the solution was filtered through Celite, ν-(CO) (CH_3CN): 2077s, 2017s cm^{-1}. The solvent was removed in vacuo leaving behind a red brown solid, with a crude yield of 0.013 g, 15.1% yield. ESI-MS (CH_3CN): {[(**Ni-1**)Rh(CO)_2]}$^+$ 420 (100%). Diffraction quality red needles were obtained by layering a concentrated CH_3CN solution with Et_2O. Anal. Calcd (found): C, 24.2 (24.5); H, 3.39 (3.49); N, 4.71 (4.83).

X-ray Diffraction Analysis: Experimental conditions for data collection and the crystal data are shown in the Supporting Information. Complete reports for structures **D** and **E** are deposited in the Cambridge Database (**D, E**: CCDC No. 291355, 291353). Low temperature (110 K) X-ray diffraction data were collected on a Bruker SMART CCD-based diffractometer (Mo K_α radiation, λ = 0.710 73 Å) and covered a hemisphere of space upon combining three sets of exposures. Structures were solved by direct methods. Programs used for data collection and cell refinement, Bruker XSCANS; data reduction, SHELXTL; absorption correction, SADABS; structure solution, SHELXS-97 (Sheldrick); structure refinement, SHELX-97 (Sheldrick); and molecular graphics and preparation of material for publication, SHELXTL-Plus, version 5.1 or later (Bruker).

Results and Discussion

Synthesis and Characterization of $[Ni(CGC)][W(CO)_4]^{2-}$ and $[Ni(CGC)][W(CO)_5]^{2-}$. According to Riordan's report,[18] we have prepared the CysGlyCys tripeptide derivative of nickel-(II), and through analogous syntheses which produced the series of NiN_2S_2 derivatives of $W(CO)_4$ and $W(CO)_5$, the $K_2[Ni$-$(CGC)W(CO)_x]$ (x = 4, 5) compounds were prepared and isolated as yellow, air-sensitive noncrystalline solids.[5,15] The potassium salt of $[Ni(CGC)W(CO)_5]^{2-}$ was also synthesized via the addition of a THF solution of $W(CO)_5(THF)$, prepared by photolysis of $W(CO)_6$ in THF, to a MeOH solution of $K_2[Ni$-$(CGC)]$. Similarly, the $[Ni(CGC)W(CO)_4]^{2-}$ complex anion was prepared in DMF solution by displacement of the labile piperidine ligands in $(pip)_2W(CO)_4$ by the thiolato donors from $K_2[Ni(CGC)]$.[19]

The $\nu(CO)$ IR bands and associated CO force constants given in Table 1 for $[Ni(CGC)W(CO)_4]^{2-}$ and $[Ni(CGC)W(CO)_5]^{2-}$ are similar to those reported for the analogous $[Ni(ema)W$-$(CO)_{4,5}]^{2-}$ complexes (see Chart 1 for abbreviations). Shown in Chart 1 are the molecular structures derived from X-ray diffraction analysis of $[Ni(ema)W(CO)_4]^{2-}$ (**A**) and the $W(CO)_5$ and $Pd(Me)Cl$ derivatives of **Ni-1**, **B**, and **C**, respectively.[15] As the $[Ni(ema)W(CO)_5]^{2-}$ compound has not been crystallized, structure **B** serves as its neutral analogue.

The comparison of the $\nu(CO)$ stretching frequencies and calculation of the Cotton−Kraihanzel force constants ranks the donor ability of the $Ni(CGC)^{2-}$ ligand with that of the dianionic NiN_2S_2 complex, $Ni(ema)^{2-}$, and better than the neutral NiN_2S_2 as ligands; the latter are in turn better electron donors toward the $W(CO)_x$ fragments than are classical diphosphine or diimine ligands, Figure 2.[15] This ranking has been extended to comparisons of $\nu(CO)$ of *o*-phenanthroline and NiN_2S_2 ligand complexes of Pd^{II} in $[(L_2)Pd(CO)(C(=O)CH_3)]^+$.[15] We conclude that $Ni(ema)^{2-}$, with its carboxyamido nitrogens and its cis
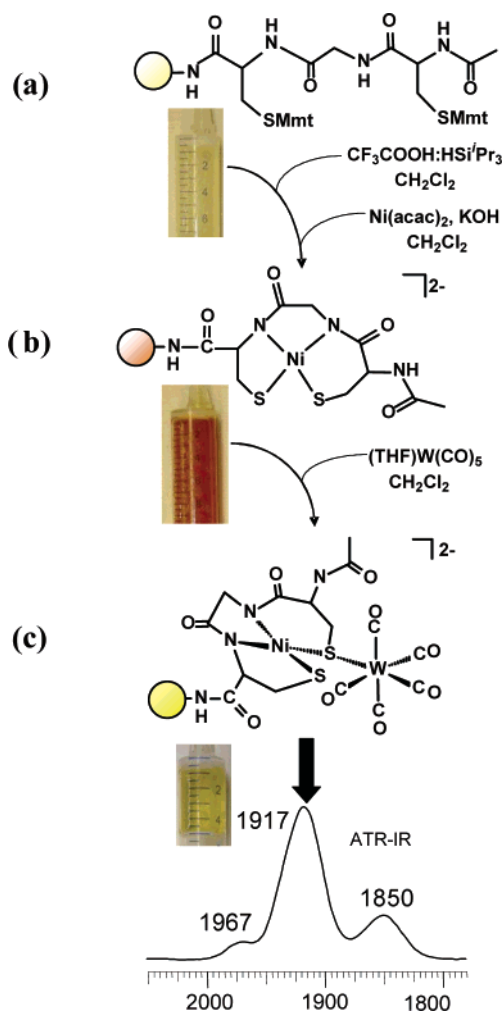
Figure 3. (a) The ○–CGC; (b) the bright orange beads consisting of ○–Ni-(CGC)$^{2-}$ suspended in CH$_2$Cl$_2$; (c) the ○–[Ni(CGC)]W(CO)$_5^{2-}$ and its ATR-FTIR spectrum.

dithiolate donors which induce a hinge effect at the bridging sulfurs, is a good model for the distal nickel, Ni$_d$, of the acetyl CoA synthase active site, Figure 1. It is similar in electron donor properties to the nickel-containing CysGlyCys tripeptide motif which supports the organometallic chemistry at the Ni$_p$.

Preparation of Resin-Bound ○–Ni(CGC)W(CO)$_5^{2-}$. Following the design of nature in the construction of the ACS active site, we strategized that the resin-bound CysGlyCys tripeptide should capture a nickel ion in N$_2$S$_2$ coordination and that this ○–Ni(CGC)$^{2-}$ might be detected by derivatization with W(CO)$_x$ ($x = 4, 5$). The TentaGel-S RAM solid support was chosen for this process as such resins are expected to contain microporous domains and they are capable of excellent swelling in a range of solvents. The latter feature is crucial to the synthesis of peptides as well as derivatives of resin-bound peptides. Thus according to the experiment depicted in Figure 3, and discussed in detail in the Experimental Section, 10 mL plastic fritted syringes were used as reaction vessels into which ca. 35 mg of TentaGel, polystyrene/poly(ethylene glycol) beads were placed. The N-acylated CysGlyCys peptide was constructed on the resin using standard Fmoc techniques. Following removal of the cysteinyl Mmt protecting group, a basic solution of Ni(acac)$_2$ in CH$_2$Cl$_2$ was introduced to the resin bed. Concomitant with bleaching of the green nickel solution, the light yellow color of

the beads developed into a bright orange. The orange beads were dried and stored in a vacuum desiccator; however limited exposure to air caused no discoloration or difference to the reactions described below.

A portion of the dry ○–Ni(CGC)$^{2-}$ was swelled with CH$_2$Cl$_2$ and exposed to a THF solution of W(CO)$_5$ whereupon the beads changed from bright orange to a burnt yellow. Several washes with CH$_2$Cl$_2$ solvent preceded vacuum-drying of the beads prior to infrared analysis. That the last wash was free of metal carbonyl was verified by its FTIR solution spectrum which showed the diatomic region (1800–2100 cm^{-1}) to be clear of absorptions. The dried beads were placed on the sample plate of the ATR-FTIR attachment. The resulting spectrum, Figure 3, showed a pattern match with THF solution phase [Ni(CGC)-W(CO)$_5$]$^-$; the position of the intense E mode is identical. The 20 cm^{-1} shift in position of the low frequency, medium intensity A$_1^2$ band, is attributed to ion-pairing effects, more operable for this band which is associated with the CO group trans to the S-donor. The high energy A$_1^1$ band of the solution complex was barely observable in the resin-bound analogue.

It should be noted that the addition of a green Ni^{II} solution to the peptide-free polystyrene resin beads, with both Fmoc protected and deprotected N-termini, resulted in no change in the color of the beads. Additionally, when (pip)$_2$W(CO)$_4$ was added to both sets of beads, no color change was observed and there were no observable ν(CO) bands. Importantly, the addition of Ni^{II} to deprotected ○–CysGly, a potentially tridentate ligand, produced deep red colored beads. Altogether these controls suggest a cysteine peptide is required for binding nickel to the resin. Furthermore, the CysGlyCys tripeptide creates an N$_2$S$_2$ ligand with similar ligating properties to that of solution Ni(CGC)W(CO)$_x^{2-}$ ($x = 4, 5$).

An interesting contrast to the reactivity of the unsupported Ni(CGC)$^{2-}$ with (pip)$_2$W(CO)$_4$ (which produces [Ni(CGC)W-(CO)$_4$]$^{2-}$) was noted as follows: When (pip)$_2$W(CO)$_4$ in CH$_2$Cl$_2$ was added to swelled ○–Ni(CGC)$^{2-}$, the ATR-FTIR spectrum acquired was identical to the one obtained when W(CO)$_5$(THF) was used as the tungsten carbonyl source. This suggests that CO is released during the synthesis, possibly by both the (pip)$_2$W(CO)$_4$ precursor and the initial product,[5,15] and the released CO is taken up by another ○–Ni(CGC)W(CO)$_4^{2-}$. This CO-scavenging reaction occurred both within the confines of the closed syringe reaction vessel and when the derivatized beads were placed in a larger Schlenk flask kept at constant (1 atm) pressure or bubbled with CO. The capture of CO leads to the thermodynamically favored pentacarbonyl product, ○–Ni-(CGC)W(CO)$_5^{2-}$, expected to be structurally similar to **B** above. Notably for both resin-bound and resin-free forms of the Ni–W complexes, there is no evidence of further substitution of the Ni(CGC)$^{2-}$ by CO to produce W(CO)$_6$. As found for neutral NiN$_2$S$_2$W(CO)$_5$ complexes, the Ni(CGC)$^{2-}$ is tenacious as a monodentate S-donor ligand to the 16-electron W(CO)$_5$ species.[5,15] The ATR-FTIR spectra of derivatized resin beads, stored as dried solids without exclusion of air, are identical to those of freshly prepared samples, indicating stability at a minimum of 2 weeks. Consistently, there is no discoloration of solvent used to swell the stored beads.

Preparation of Resin-Bound ○–Ni(CGC)Rh(CO)$_2^-$. Further derivatization of the resin-bound Ni tripeptide has been directed toward metal carbonyl moieties of potential catalytic

ability. Analogous to diimine and diphosphine derivatives,[21] neutral NiN$_2$S$_2$ ligands form Ni—Pd binuclear complexes of Pd^{II}-(CH$_3$)$_2$ or Pd^{II}(CH$_3$)(Cl), structure **C**, which exhibit organometallic reactivity of CO addition and insertion characteristic of the CO/olefin copolymerization catalysis of polyketone.[15] The rhodium(I) dicarbonyl unit, chelated by bidentate diimine or diphosphine ligands, is also known to catalyze a range of processes including intramolecular hydroamination,[22,23] decarbonylation,[24] and carbonylation of methanol.[25–27] As an analogue to the Pd complexes, Rh^I(CO)$_2^+$ derivatives of Ni(CGC)$^{2-}$ were pursued.

Addition of a CH$_2$Cl$_2$ solution of [Rh(CO)$_2$Cl]$_2$ as the source of Rh^I(CO)$_2^+$ to samples of the solvent-swelled O—Ni(CGC)$^{2-}$ led to an immediate change in the orange color of the beads to a dark purple/brown hue. Upon washing with CH$_2$Cl$_2$ and drying as described before, the ATR-FTIR spectrum of the beads revealed two sharp bands of equal intensity at 2067 and 1990 cm^{-1}, indicative of the A$_1$ symmetric and B$_1$ asymmetric vibrational modes of the cis-CO groups at 90° angles ($I_a/I_s =$ tan^2 θ) as would be expected for a square planar S$_2$Rh(CO)$_2$ unit within the O—Ni(CGC)Rh(CO)$_2^{-1}$ bimetallic complex.[28]

The ability of NiN$_2$S$_2$ to bind to Rh(CO)$_2^+$ was corroborated by synthesis of solution analogues that might be amenable to isolation and crystal structure analysis. On mixing of acetonitrile solutions of the red [Rh(CO)$_2$Cl]$_2$ dimer and the dark red [NEt$_4$]$_2$[Ni(ema)] compound, a purple/brown solution developed within an hour. The ν(CO) IR spectrum of this solution exhibited two sharp bands of equal intensity at 2063 and 1992 cm^{-1}, consistent with the expected [NEt$_4$][Ni(ema)Rh(CO)$_2$] product and similar in pattern and position to the solid-state IR spectrum of O—Ni(CGC)Rh(CO)$_2^-$. The negative mode of ESI-MS corroborated the presence of Ni(ema)Rh(CO)$_2^-$ via the appropriate isotopic bundle at 421 *m/z*. The analogous cationic complex based on the neutral NiN$_2$S$_2$ complex, [(**Ni-1**)Rh(CO)$_2$]-[PF$_6$], was similarly prepared by addition of [Rh(CO)$_2$Cl]$_2$ to **Ni-1** in CH$_3$CN. The symmetrical two-band ν(CO) IR absorbances for the red-orange [(**Ni-1**)Rh(CO)$_2$]$^+$ are positioned at 2085 and 2017 cm^{-1}. The significant shift to higher frequencies as compared to [NEt$_4$]$_2$[Ni(ema)Rh(CO)$_2$]$_2$ and the O—Ni-(CGC)Rh(CO)$_2^-$ is consistent with the charge differences in the cationic vs anionic derivatives.

Both the [Et$_4$N]$_2$[Ni(ema)Rh(CO)$_2$]$_2$ and [(**Ni-1**)Rh(CO)$_2$]-[PF$_6$] salts were crystallized and subjected to X-ray diffraction analysis. The solid-state structures are given as thermal ellipsoid plots in Figures 4 and 5 along with ball-and-stick drawings of alternative views. In both structures the Rh^I is in S$_2$(CO)$_2$ square planar coordination with cis CO groups. The [(**Ni-1**)Rh(CO)$_2$]$^+$ cation is a simple heterobimetallic with a single NiN$_2$S$_2$ unit serving as a bidentate ligand to Rh^I in the same manner as the
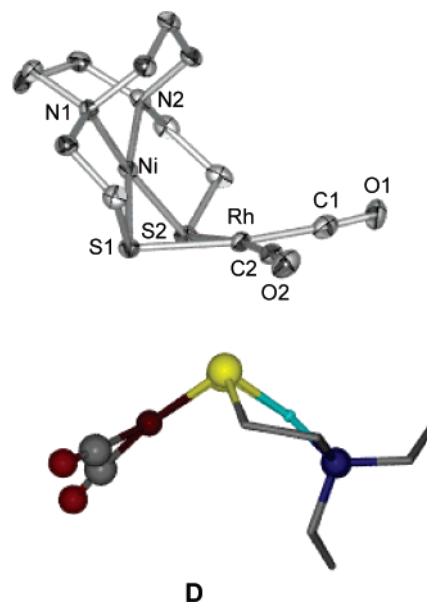
(20) Cotton, F. A.; Kraihanzel, C. S. *J. Am. Chem. Soc.* **1962**, *84*, 4432–4438.
(21) van Leeuwen, P. W. N. M.; Kamer, P. C. J.; Reek, J. N. H.; Dierkes, P. *Chem. Rev.* **2000**, *100*, 2741–2769.
(22) Burling, S.; Field, L. D.; Messerle, B. A.; Turner, P. *Organometallics* **2004**, *23*, 1714–1721.
(23) Burling, S.; Field, L. D.; Li, H. L.; Messerle, B. A.; Turner, P. *Eur. J. Inorg. Chem.* **2003**, 3179–3184.
(24) Del Zotto, A.; Costella, L.; Mezzetti, A.; Rigo, P. *J. Organomet. Chem.* **1991**, *414*, 109–118.
(25) Rankin, J.; Poole, A. D.; Benyei, A. C.; Cole-Hamilton, D. J. *Chem. Commun.* **1997**, 1835–1836.
(26) Dilworth, J. R.; Miller, J. R.; Wheatley, N.; Baker, M. J.; Sunley, J. G. *Chem. Commun.* **1995**, 1579–1581.
(27) Baker, M. J.; Giles, M. F.; Orpen, A. G.; Taylor, M. J.; Watt, R. J. *Chem. Commun.* **1995**, 197–198.
(28) Manning, A. R. *J. Chem. Soc. A* **1967**, 1982–1987.

D

Figure 4. Two views of [(**Ni-1**)Rh(CO)$_2$]$^+$, **D**, represented by a thermal ellipsoid plot as well as a ball-and-stick drawing; PF$_6^-$ anion excluded.

E

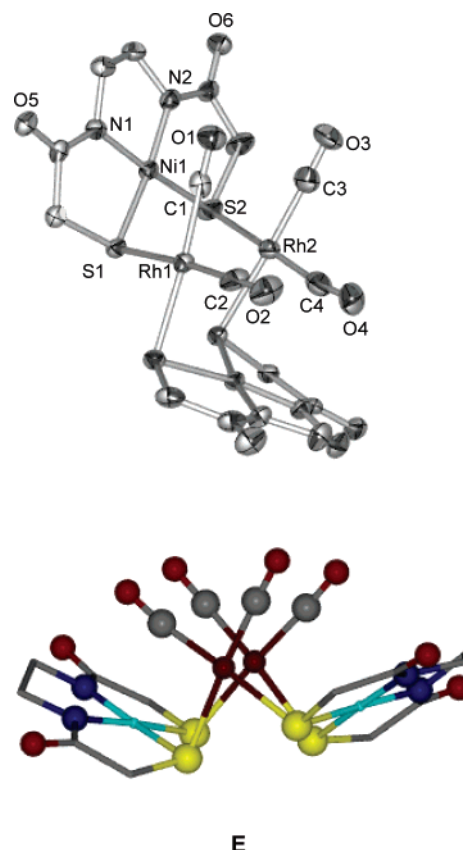**Figure 5.** Two views of [(Ni-ema)Rh(CO)$_2$]$_2^{2-}$, **E**, represented by a thermal ellipsoid plot and a ball-and-stick drawing, with Et$_4$N$^+$ cations excluded.

NiPd complex, structure **C** above.[15] The Ni(ema)$^{2-}$ derivative, however, crystallizes as a tetrametallic in which two Ni(ema)$^{2-}$ units serve as bidentate bridges to two Rh(CO)$_2^+$ components. The two S$_2$Rh(CO)$_2$ planes in **E** are largely eclipsed with a slight deviation resulting in SRhRhS torsion angles averaging 16°, Figure S1. The two S$_2$Rh(CO)$_2$ planes are also, for the most part, parallel. The extrapolated intersection of these two planes is 3.7°.

The intersection of NiN_2S_2 and $RhS_2(CO)_2$ square planes of cation **D** is 106°, which is slightly larger than the 101° angle found in the (**Ni-1**)Pd(Me)Cl structure **C** above. An analogous hinge angle is defined for the tetrametallic structure **E** as the intersection of a NiN_2S_2 plane with the best plane defined by S_2Rh_2. This turns out to be 107.4° and 98°; as the two NiN_2S_2 units arrange to produce different angles with the dirhodium core.

There are minor differences in the metric data between the free and bound NiN_2S_2 ligand. The $\angle_{S-Ni-S}$ of 84.65(3)° is slightly smaller in compound **D** than that of the free ligand, i.e., **Ni-1**, which is 89.4(1)°. The analogous angles in compound **E** and its free ligand ($Ni(ema)^{2-}$) are 98.82(5)° and 97.44(8)°. The greater rigidity of $Ni(ema)^{2-}$ coupled with its larger bite angle may account for the preference for binding in a bidentate bridging mode. It should be mentioned that the $S_2Rh(CO)_2$ units in **E** show less deviation from the 90° angles of regular square planarity as compared to structure **D**.

Altogether these results lead to the conclusion that the ◯−Ni-$(CGC)^{2-}$ binds to $Rh(CO)_2$ producing an $S_2Rh(CO)_2$ unit. While the precise morphology of the resin and relative positioning of the resin-bound metalloligands are unknown, other groups have shown that polystyrene/poly(ethylene glycol) based resins form microdomains in which site isolation is prescribed.[7,29] Based on this characteristic of the support utilized in our work, it is reasonable to assume that site isolation will limit aggregation and produce a complex similar to **D**. Although it is not clearly understood, the stabilization of resin-bound organometallic complexes has been noted.[6,8,29] In our case, the prevention of deleterious reactions may be attributed to these microdomains formed by the poly(ethylene glycol) tentacles of the TentaGel resins.[7,30] Nevertheless in both the heterobimetallic and the heterotetrametallic $[(NiN_2S_2)Rh(CO)_2]_x$ complexes ($x = 1,2$) the S donors produce a ligand field about Rh^I that reflects the donor ability of the respective NiN_2S_2 ligands. Interestingly, the sulfur donors from the dianionic NiN_2S_2, $[Ni(ema)Rh(CO)_2]^-$ or ◯-Ni-$(CGC)^{2-}$, create a $Rh(CO)_2^+$ moiety that has electronic properties similar to those of $Rh(CO)_2I_2^-$ ($\nu(CO)$ values of 2059 and 1988 cm^{-1}),[25] which is a catalyst precursor for the Monsanto Acetic Acid Process. Notably, the industrial catalysis invokes the same key steps of methyl oxidative addition, CO insertion, and ultimately reductive elimination, a process very similar to the mechanism of ACS.[4] The catalytic potential of ◯−Ni(CGC)-$Rh(CO)_2^-$ and solution analogues awaits exploration.

Supporting Information Available: The crystallographic data for structures **D** and **E** have been deposited into the Cambridge Database, CCDC No. 291355 and 291353, respectively. This material is available free of charge via the Internet at http://pubs.acs.org.

JA060876R

(29) Annis, D. A.; Jacobsen E. N. *J. Am. Chem. Soc.* **1995**, *117*, 4147−4154.

(30) Bayer, E. *Angew. Chem., Int. Ed. Engl.* **1991**, *30*, 113-216.